Oxygen-Bound Fluorine (O−F): *Ab Initio* Investigations of the Hypofluorous Acid Dimer

Sławomir Berski,[†] Jan Lundell,[‡] Zdzisław Latajka,*[,†] and Jerzy Leszczyński[§]

Faculty of Chemistry, University of Wrocław, 14 F. Joliot-Curie, 50-383 Wrocław, Poland, Laboratory of Physical Chemistry, University of Helsinki, P.O. Box 55 (A. I. Virtasen Aukio 1), FIN-00014 Helsinki, Finland, Department of Chemistry, Jackson State University, P.O. Box 17910, Jackson, Mississippi 39217

Received: May 8, 1998; In Final Form: October 16, 1998

Ab initio calculations have been carried out on dimers of hypofluorous acid−$(HOF)_2$. Two stable structures were found, the first one with an almost linear O···H−O hydrogen bridge and F···H−O hydrogen bond and the second one being a cyclic dimer with two F···H−O bonds. The most stable complex determined at the CCSD(T)/6-311++G(2d,2p)//MP2/6-311++G(2d,2p) level is the linear structure, having a stabilization energy of 2.50 kcal/mol. The cyclic structure is only 0.35 kcal/mol higher in energy than the linear one. The organization of the attractors achieved by the topological analysis of the electron localization function (ELF) classifies the interaction in both dimer structures as the unshared-electron type. A transfer of 0.03e between the HOF monomers in the linear structure is deduced from the comparison of the basin populations. The integral density over the F−O attractor basins yields 0.32e for the cyclic structure and 0.27 and 0.37 e for the linear one. The large amount of electron density is concentrated in the regions of the nonbonding valence pairs. The influence, which a dielectric surrounding has on the HOF dimers, has been investigated with the SCRF method, with dielectric constants ranging from 2 to 10 at the B3LYP/6-31G(d,p) level. The cyclic structure which assumed planar (C_{2h}) geometry was found to be unstable (transition state) within a dielectric medium. The calculated frequencies for the linear complex (C_1) agree reasonably well with those observed in a matrix, particularly in the H−O−F deformation region between 1365−1396 cm^{-1}.

I. Introduction

The hypohalous acids (HOX, X = F, Cl, Br, or I) are important atmospheric compounds, which are assumed to play an important role in the ozone depletion reactions.[1−7] The hypochlorous (HOCl) and hypobromous (HOBr) acids are trace gases in the stratosphere, whereas the hypoiodous acid (HOI) has been suggested to be involved in the tropospheric iodide chemistry.[8]

All hypohalous acids are powerfull oxidants. The 1:1 adduct between hypofluorous acid (HOF) and acetonitrile (CH_3CN) has been proposed as a powerful oxygen-transfer agent.[9,10] The reactive hydroxylium moiety ($HO^{\sigma+}$) is responsible for unprecedentedly fast epoxidations and hydroxylations. Dunkelberg et al.[11] elucidated the crystal structure of the CH_3CN−HOF adduct by low-temperature X-ray diffraction. The length of a linear, intermolecular hydrogen bond between N and H was established to be 1.7 Å.

The HOF molecule is relatively well characterized by IR,[11,12] microwave,[13] photoelectron,[14] photoionization,[15] and ^1H and ^{19}F NMR[16] spectra. Its chemical properties reflect an interplay between a highly electronegative F atom (σ-inductive role) and repulsive interactions between the electron lone pairs of the oxygen and fluorine atoms. The most prominent feature of hypohalous acids is their instability.

Experimental evidence for HOF oligomers was presented by Appelman et al.,[17] who assigned $(HOF)_2$ and $(HOF)_3$ complexes to bands observed in the infrared spectra of hypofluorous acid trapped in solid matrices. The vibrational properties of $(HOF)_2$ appeared to resemble those of $(HF)_2$ and suggested that for $(HOF)_2$ in low-temperature matrices, a linear structure was favored.

Recently, Poll et al.[18] carried out an X-ray structure analysis of pure HOF in the condensed phase and obtained a crystal structure exhibiting $(HOF)_\infty$ chains with almost linear O···H−O hydrogen bonds. The previous assumption based on IR and Raman spectroscopic studies by Appelman et al.[19] and Kim et al.[20] lead to an interpretation with planar zigzag chains of F···H−O hydrogen bonds. The theoretical proof of the greater probability of O···H−O bonds was done by Christe[21] on the basis of two pieces of information.

First, *ab initio* calculations at the Hartree−Fock level with a minimal basis set suggested that oxygen is more net negative (−0.210 e) than fluorine (−0.122 e).[22] However, it must be emphasized that the adopted computational level seems to be inadequate, and even at the MP2/6-311++G(3df,3pd) level, the Mulliken population analysis (MPA) and natural population analysis (NPA) yield unrealistic atomic charges, i.e., fluorine less negative than oxygen.[23] Recently, we showed that the correct atomic charges (in accordance to values of electronegativities by Allred and Rochow[24]) can be computed at the MP2/6-311++G(3df,3pd) level using 6d and 10f Cartesian functions.[23] The net charges of −0.23 and −0.12 e for fluorine and oxygen, respectively, were in excellent agreement with the values of −0.23 and −0.15 e obtained using Bader's (AIM) method.[25]

Second, the quantum-mechanical study on the proton affinities of oxygen and fluorine favored oxygen by 12 kcal/mol.[26] Alcamí et al.[27] predicted at the HF/6-31G(d) and 6-31+G(d,p) levels the differences to be 15.9 and 15.2 kcal/mol, respectively. Burk et al.[28] using G2 theory at the MP2 and CISD/6-31G(d) levels,

* Corresponding author.
[†] University of Wrocław.
[‡] University of Helsinki.
[§] Jackson State University.

10.1021/jp982189v CCC: $15.00
Published on Web 12/09/1998

found the protonation on the O atom to be more favorable by 18 kcal/mol.

Therefore, an explanation between the competing OH···F and OH···O hydrogen bonds based on the net atomic charges and the proton affinities of F and O obtained from *ab initio* calculations cannot be answered in a straightforward manner. In this context, our study on hypofluorous acid dimers may give some view on the relative hydrogen-bonded ability of acceptors.

In this work, we present a theoretical study of the structure, vibrational properties, and energetics of dimers formed by hypofluorous acid. We will show that the existence of both types of intermolecular H bonds is almost equally feasible. Furthermore, we use a very modern analysis of the bonding based on the topological analysis of the electron localization function (ELF) proposed by Silvi and Savin[29] in order to investigate the redistribution of the electron density in $(HOF)_2$. The effect of surrounding molecules was considered by the self-consistent reaction field (SCRF) approximation, and the obtained infrared data were compared with the results of the IR experiments in solid rare gas matrices.

II. Computational Details

Structures of HOF monomers and dimers were evaluated at the second-order perturbation theory levels (MP2). Additionally, density functional theory (DFT) calculations were performed within the B3LYP approximation where the Becke exchange functional[30] is coupled with the Lee−Yang−Parr correlation.[31] The standard 6-31G(d,p)[32] and 6-311++G(2d,2p)[33] basis sets were used for geometry optimizations. The stationary points were characterized by frequency calculations. The interaction energy was calculated as the difference of the total energy between the dimer and the monomers at infinite distance, where the monomer wave functions were derived in the dimer-centered basis set (DCBS). This aproach corresponds to the counterpoise correction proposed by Boys and Bernardi[34] aimed to minimize the basis superposition error (BSSE) in the interaction energy. The dimer energetics were also evaluated by calculations at the coupled cluster CCSD(T)/6-311++G(2d,2p)//MP2/6-311++G-(2d,2p) single-point level. All interaction energies were corrected by the zero vibrational energies (ZPEs). The calculations were carried out with the GAUSSIAN 94 program package.[35] The topological analysis of the electron localization function (ELF) was performed with the ELFGTO program[36] using wave functions generated at the B3LYP/6-311++G(2d,2p) level.

III. Results and Discussion

Structure. Two minimum energy structures of the $(HOF)_2$ complex with different geometries were found. The first one is an almost planar, cyclic conformation with two F···H−O hydrogen bonds and is of C_2 point group of symmetry (it is described as C_2). The second one is nonplanar of C_1 symmetry, and it differs by the orientation of one of the HOF subunits. There are two hydrogen bonds of the O···H−O and F···H−O types within the dimer (described as C_1). The optimized $d(H_3\cdot\cdot\cdot F_4)$ distances of 2.541 (MP2) and 2.427 Å (B3LYP) suggest that a very weak hydrogen bond between the OH group and the F atom exists. The optimized structures are shown in Figure 1.

In the cyclic structure (C_2), the distances between the hypofluorous acid molecules are 2.021 (MP2) and 1.991 Å (B3LYP), and the deviation from a linear F···H−O bond is slightly smaller at the B3LYP level (32.2°) than at MP2 (34.2°). Upon complex formation, rather small elongations of the O−H and F−O bonds are found, only 0.004 and 0.006 Å at the MP2 and B3LYP levels, respectively. This observation is in agreement with the report by Glukovtsev et al.[37] that the O−F bond becomes longer when a protonation takes place at the more electronegative atom. At the same time, the intramolecular H−O−F angle decreases by 0.2° (MP2) and 0.4° (B3LYP), respectively. The cyclic complex is slightly nonplanar, and the nonplanarity of $(HOF)_2$ is presented by the $O_2-F_1-H_6-O_5$ dihedral angle which is 31.9° and 20.3° at the MP2 and B3LYP levels of theory, respectively.

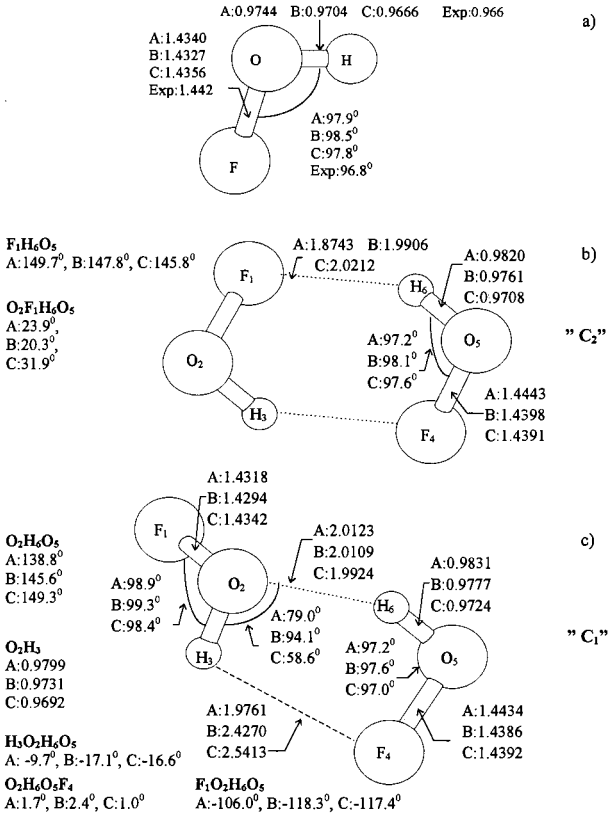

Figure 1. Optimized structures of (a) FOH (C_s), (b) the $(FOH)_2$ minimum energy complex with cyclic conformation (C_2), (c) the $(FOH)_2$ minimum energy complex with linear conformation (C_1) computed at the (A) B3LYP/6-31G(d,p), (B) B3LYP/6-311++G(2d,2p), and (C) MP2/6-311++G(2d,2p) levels. The experimental data are from ref 48.

For the linear dimer structure (C_1), the MP2/6-311++G(2d, 2p) level predicts a bent $O_5H_6\cdot\cdot\cdot O_2$ hydrogen bond with deviation from linearity by 30.70°. At the B3LYP/6-311++G-(2d,2p) level, the same angle is predicted to be 34.4°. The hydrogen bond length to the O_2 atom is 1.9924 (MP2) and 2.0109 Å (B3LYP). These values indicate that the $O_5H_6\cdot\cdot\cdot O_2$ hydrogen bond is shorter by 0.0288 Å than the $O_5H_6\cdot\cdot\cdot F_1$ hydrogen bond at the MP2 level but slightly larger (0.0203 Å) at the B3LYP level of theory. The complexation induces small perturbation in the monomer geometries. The formation of the hydrogen bonds lengthens the O_5H_6 bond about 0.006 (MP2) and 0.007 Å (B3LYP) and the F_4O_5 bond about 0.004 (MP2) and 0.006 Å (B3LYP). For the other HOF subunit ($H_3O_2F_1$) in the linear dimer, the F_1O_2 is contracted about 0.001 (MP2) and 0.003 Å (B3LYP). This is due to the-donor−acceptor nature of the linear dimer as will be discussed below based on the ELF analysis.

Energetics. The calculated B3LYP/6-31G(d,p), B3LYP/6-311++G(2d,2p), and MP2/6-311++G(2d,2p) total energies, zero-point energies, BSSE values, and relative energies of the two stable structures of $(HOF)_2$ and the isolated hypofluorous acid (HOF) are collected in Table 1. For comparison, single-

TABLE 1: Calculated Energetics of the Linear and Cyclic Conformers of the $(HOF)_2$ Complex

	B3LYP/6-31G(d,p)		MP2/6-311++G(2d,2p)		B3LYP/6-311++G(2d,2p)		CCSD(T)/6-311++G(2d,2p)d)[a]	
species	ZPE[a]	*E*	ZPE	*E*	ZPE	*E*	ZPE[c]	*E*
HOF	8.76	−175.527 675	8.82	HF: −174.794 002 MP2: −175.256 456	8.76	−175.601946	8.82	−175.277265
dimer C_1	19.5	−351.068 328	19.3	HF: −349.593 537 MP2: −350.521 230	19.1	−351.211693	19.3	−350.563000
dimer C_2	19.5	−351.071 010	19.4	HF: −349.594 888 MP2: −350.521 359	19.1	−351.211778	19.4	−350.563920

species	interaction energies, kcal/mol			
dimer C_1				
ΔZPE[b]	1.98	1.66	1.58	1.66
ΔE	−8.15	−5.22	−4.57	−5.89
BSSE	3.77	1.31	0.59	1.73
$\Delta E^{CP} + \Delta$ZPE	−2.40	−2.25	−2.39	−2.50
dimer C_2				
ΔZPE	1.98	1.76	1.58	1.76
ΔE	−9.83	−5.30	−4.95	−5.32
BSSE	4.56	1.57	0.65	1.40
$\Delta E^{CP} + \Delta$ZPE	−3.29	−1.97	−2.72	−2.16

[a] Zero-point energy in kcal/mol. [b] Zero-point energy difference between the complex and the isolated monomers. [c] Zero-point energy at the MP2/6-31++G(2d,2p) level. [d] The optimized geometry from MP2/6-311++G(2d,2p) level was used.

point calculations at the CCSD(T)/6-311++G(2d,2p) level using the MP2/6-31 1++G(2d,2p)-optimized geometry were performed.

The results in Table 1 indicate that the relative stability difference between the linear and cyclic structures is very small and depends on the computational methodology. The linear complex of $(HOF)_2$ is more stable at the MP2/6-311++G(2d, 2p) and CCSD(T)/6-311++G(2d,2p)//MP2/6-311++G(2d,2p) levels. The differences in the complexation energy are of the order of 0.28 and 0.34 kcal/mol, respectively, compared with the less stable cyclic structure. For the DFT calculations at the B3LYP/6-31G(d,p) and B3LYP/6-311++G(2d,2p) levels, the cyclic structure of hypofluorous acid is 0.89 and 0.33 kcal/mol more stable than the linear one.

A zero-point energy difference (ΔZPE) between the complex and the isolated monomers reduces generally the complexation energy (ΔE^{CP}) by about 40%. Because the BSSE may essentially influence the potential energy surface of the hydrogen-bonded complexes, the interaction energies were corrected by the counterpoise technique (CP) proposed by Boys and Bernardi.[34] The fragment relaxation energy terms in the estimation of the CP were included, and the details of this procedure may be found in the recent study of Xantheas.[38] It is interesting to note that the BSSE is about 50% smaller in the case of the B3LYP/6-311++G(2d,2p) level than at the MP2/6-31++G(2d,2p) and CCSD(T)/6-311++G(2d,2p)//MP2/6-311++G(2d,2p) levels. The CP reduces the complexation energy about 30% for the MP2 and CCSD(T) computations but only by 13% at the B3LYP/6-311++G(2d,2p) level. There are additional data of the B3LYP/6-31G(d,p) energetics computed for $(HOF)_2$ in Table 1.

The analysis of the physical properties of the HOFs may be related to hydrogen fluoride (HF), and the vibrational properties of the $(HOF)_2$ complexes resemble those of $(HF)_2$. Moreover, calculations at the MP2/6-311++G(2d,2p) level yield comparable values for the ΔE and ΔE^{CP} energies, i.e., −4.86 and −3.84 kcal/mol for $(HF)_2$, presented by Novoa et al.[39] In comparison, we predict −5.22 and −3.91 kcal/mol for the linear and −5.30 and −3.73 kcal/mol for the cyclic $(HOF)_2$ structures. Also, the $(HOF)_2$ complexes may be compared to the water dimer. Studying the ΔE and ΔE^{CP} values for the linear and cyclic geometries of $(HOH)_2$, i.e., −5.41 and −4.43 kcal/mol, respectively,[39] suggests that the energetics of the water dimer resemble $(HOF)_2$ better than $(HF)_2$, particularly when BSSE uncorrected values of ΔE are considered. Nevertheless, the comparison of the ΔE^{CP} values yields better agreement between the $(HOF)_2$ and $(HF)_2$ complexes than between the $(HOF)_2$ and $(H_2O)_2$ dimers. This behavior is consistent with our chemical intuition based on the observation that HOF possesses a structure which is intermediate between those of HOH and HF. The other possible comparison of $(HOF)_2$ may be the one with the HOH−HF complex. However, the computed[39] ΔE and ΔE_{CP} values of −9.35 and −7.90 kcal/mol, respectively, are about 50% larger than those found in our study on $(HOF)_2$. Thus, the energetics of HOH−HF must differ substantially from those of $(HOF)_2$.

Vibrational Frequencies and Intensities. The vibrational spectra of the monomer and dimers were analyzed in the framework of the 6-311++G(2d,2p) basis set at the B3LYP and MP2 levels of calculations. Taking the fully optimized geometry at the appropriate level of calculations as a reference point, the frequencies and intensities were computed by the double-harmonic approximation.

The vibrational spectrum computed for the isolated FOH molecule is reported in the first three rows of Table 2. ν_1 and ν_3 correspond to OH and OF stretching, respectively, whereas ν_2 describes the FOH bending mode. The frequencies and intensities are not too sensitive to the method used in the calculations.

The remaining rows in Table 2 describe the calculated frequencies and intensities of different dimers. As in the majority of hydrogen-bonded systems, the vibrational modes of the isolated monomers remain largely recognizable as intramolecular modes in the complex. A comparison of the vibrational modes of the dimers to the corresponding modes of the isolated monomer reveals that there are significant shifts due to the complexation. Most affected by the formation of the hydrogen bond is the O−H stretching mode. The two O−H stretching vibrations of the linear dimer (C_1), located at 3711.4 and 3611.3 cm^{-1}, respectively, are red-shifted by 27.4 and 101.4 cm^{-1}, respectively, at the MP2 level. The large red shift of 101.4 cm^{-1} for the O_5H_6 bond stretching indicates a stronger $O_5H_6\cdots F_1$ hydrogen bridge. Corresponding values of red shifts calculated at the B3LYP level are slightly larger. In addition to the large red shift of the O−H stretching mode, there is also an increase of intensity observed compared to the isolated monomer.

For the cyclic dimer (C_2), at the MP2 level, the red shifts

TABLE 2: Vibrational Frequencies (ν, in cm^{-1}) and Intensities (I, in km/mol) of the HOF Monomer and Cyclic (C_2) and Linear (C_1) HOF Dimers Calculated with the 6-311++G(2d,2p) Basis Set

	B3LYP		MP2		
	ν	I	ν	I	approx assignment
			Monomer		
ν_1[a]	3744.4	49.1	3797.2	48.8	OH str
ν_2	1414.3	55.4	1416.8	63.6	FOH bend
ν_3	970.0	9.3	955.0	1.4	OF str
			Dimer C_1		
ν_1[a]	3711.4	83.0	3769.8	79.6	O_2H_3 str
ν_2	3611.3	243.7	3695.8	242.1	O_5H_6 str
ν_3	1475.6	62.4	1480.9	65.1	$F_4O_5H_6$ bend
ν_4	1412.4	62.1	1413.1	66.0	$F_1O_2H_3$ bend
ν_5	978.1	8.5	956.6	1.1	F_1O_2 str
ν_6	955.9	11.3	955.5	1.9	F_4O_5 str
ν_7[b]	482.2	146.5	499.3	136.5	$F_4O_5H_6$ wag
ν_8	346.8	104.9	334.4	112.8	$F_1O_2H_3$ wag
ν_9	178.2	25.3	190.3	22.9	$F_4O_5H_6$ wag
ν_{10}	94.7	35.3	89.0	29.8	$F_1O_2H_3$ wag
ν_{11}	62.0	5.4	58.2	4.5	intermolec str
ν_{12}	41.2	7.7	34.2	7.4	torsion
			Dimer C_2		
ν_1[a]	3664.3	318.9	3747.5	264.6	out-of-phase OH str
ν_2	3638.0	0.6	3727.4	2.5	in-phase OH str
ν_3	1483.3	8.9	1481.9	22.7	out-of-phase FOH bend
ν_4	1451.9	129.9	1448.4	121.3	in-phase FOH bend
ν_5	953.5	26.4	959.2	0.5	out-of-phase FO str
ν_6	950.1	2.1	957.3	4.4	in-phase FO str intermolec modes
ν_7[b]	431.1	202.2	450.3	154.4	out-of-phase out-of-plane bend
ν_8	272.5	38.4	257.2	96.5	in-phase out-of-plane bend
ν_9	176.8	51.5	172.0	43.8	out-of-phase in-plane bend
ν_{10}	156.6	7.1	147.6	5.1	in-phase in-plane bend
ν_{11}	147.8	0.1	144.8	4.5	intermolec str
ν_{12}	40.1	0	59.1	0	torsion

[a] Intramolecular modes. [b] Intermolecular modes.

are as large as 49.7 and 69.8 cm^{-1} for the out-of-phase and in phase O−H stretching modes, respectively. Considerable frequency shifts are also noted for the FOH bending modes. For example, a blue shift of 64.1 cm^{-1} (at the MP2 level) is noted for the $F_4O_5H_6$ bending mode of the linear dimer. Also, a similar large blue shift of 65.1 cm^{-1} is calculated for the out-of-phase FOH bending mode of the cyclic dimer. The FO stretching modes are predicted to be close to the monomer fundamental and are less perturbed by the dimer formation. For the calculated intensities, the effect of complexation is mostly noted for the O−H stretching modes of both dimers. The intensities of the remaining intramolecular modes are less affected.

The intermolecular, low-frequency modes are probably quite anharmonic, and the calculated harmonic wavenumbers give only an approximate picture of them. Nevertheless, *ab initio* calculations can play a particularly important role in the prediction and interpretation of this portion of the spectrum. In all cases, the highest frequency vibrations are predicted to be the out-of-plane wags, and relatively high intensities characterize these modes. The frequencies of the intermolecular stretching modes of both complexes (ν_{11}) are fairly low and are around 60 and 145 cm^{-1} for the linear and the cyclic dimer, respectively. The final mode (ν_{12}) corresponds to a torsional motion and is of very low frequency and intensity for both dimers.

Interactions in the $(HOF)_2$ Complexes. As was mentioned in the Introduction, the Mulliken population analysis (MPA) does not describe correctly the distribution of the electron density in $(HOF)_2$, which should correspond to the values of electronegativities by Allred and Rochow[24] (4.1 for fluorine and 3.5 for oxygen). The computations at the MP2/6-311++G-(2d,2p) level show net atomic charges of −0.03, −0.25, and 0.28 e for F, O, and H, respectively. Similar results can be achieved using the DFT approximation. Recently, Lee et al.[40] investigated the varying nature of fluorine−oxygen bonds at the CCSD(T)/TZ2P level of theory. The MPA and the electrostatic potential (CHELP method[41]) methods predicted partial atomic charges of −0.15/−0.20 e (MPA) and −0.10/−0.28 e (CHELP) for fluorine and oxygen in HOF, respectively. Similarly, for FOBr, values of −0.12/−0.16 e (MPA) were found for bromine and oxygen. Therefore, we will only consider the topological analysis of the ELF in this study.

Recently, the role of the electron density was emphasized by Bader's theory[42] of atoms in molecules (AIM) model, which is in an alternative to the different population analysis schemes (Mulliken, Löwdin, Mayer, NPA). Its complementary and augmenting character was recently elaborated by Silvi and Savin,[29] who took advantage of the idea of ELFs of Becke and Edgecomb.[43] ELF can be considered as a measure of the Pauli repulsion, and it is defined as

$$\mathrm{ELF} = \frac{1}{1 + \left[\frac{D_\sigma(x,y,z)}{D_\sigma^0(x,y,z)}\right]^2}$$

where D_σ and D_σ^0 represent the curvature of the electron pair density for electrons of identical spin (Fermi hole) for the actual system and a homogenous electron gas with the same density, respectively. In this approach, D_σ can be identified as the Pauli kinetic energy density of the actual fermionic system with respect to a bosonic system having the same density. Therefore, ELF is a measure of the bosonic behavior of the electron density. The ELF function is actually defined for a system with electron density $\rho(x,y,z)$ using a single determinental wave function built from Hartree−Fock or Kohn−Sham orbitals φ_i, with

$$D_\sigma = \frac{1}{2}\sum_i |\nabla\varphi_i|^2 - \frac{1}{8}\frac{|\nabla\rho(x,y,z)|^2}{\rho(x,y,z)}$$

$$D_\sigma^0 = \frac{3}{10}(3\pi^2)^{5/3}\rho^{5/3}$$

and calculated on a grid in the three-dimensional space. By definition, ELF runs from 0 to 1 and is equal to 0.5 for homogeneous electron gas.

The classification of chemical bonds is based on the presence of point, ring, and spherical attractors. From a chemical point of view, there are three types of attractors: the core, bonding which is located between the core attractors, and nonbonding attractors. The number of cores connected to a given valence attractor determines its synaptic order. The integration of the electron density over the basin of a given attractor. allows us to compute the average electron population of cores, bonds, or lone pairs,

$$N(\Omega_A) = \int \rho(\mathbf{r})\, d\mathbf{r}$$

where Ω_A refers to a basin attractor, $N(\Omega_A)$ is a mean electron population, and $\rho(\mathbf{r})$ is electron density.

Following Bader,[44] there are basically two kinds of bonding interactions: shared-electron interaction and closed-shell interaction. Covalent, dative, and metallic bonds are subclasses of the shared-electron interaction, whereas ionic, hydrogen, electrostatic, and van der Waals bonds belong to the other class. For shared-electron interaction, there is always at least one bond

TABLE 3: ELF-Basin Populations for the Cyclic (C_2) and Linear (C_1) Conformations of the $(HOF)_2$ Complex Calculated at the B3LYP/6-311++G(2d,2p) Level

ELF results[a]	$\acute{N}$ FOH isolated[b]	$\acute{N}$ $(FOH)_2$ cyclic	$\acute{N}$ $(FOH)_2$ linear
atomic core attractors			
C_1 (F_1)	2.13	2.15	2.15
C_2 (O_2)	2.12	2.13	2.13
C_3 (F_4)		2.15	2.17
C_4 (O_5)		2.13	2.11
lone pair monosynaptic attractors			
V_1 (O_2)	4.70	4.69	4.91
V_2 (F)	6.77	6.87	6.85
V_3 (O_5)		4.69	4.66
V_4 (F_4)		6.87	6.83
protonated disynaptic attractors			
V_1 (O_2, H_3)	1.78	1.80	1.65
V_2 (O_5, H)		1.80	1.85
F−O bonding disynaptic attractors			
V_3 (F_1, O_2)	0.42	0.32	0.27
V_4 (F_4, O_5)		0.32	0.37

[a] The attractors and their basins are labeled as $T_{[i]}$ (atom labels). "T" denotes the type of attractor ("*C*", core; "V, valence); "*i*" is a running number. For instance, $V_3(F_I,O_2)$ describes the disynaptic attractor of the F_1-O_2 bond which is numbered as the third one. [b] From ref 48.

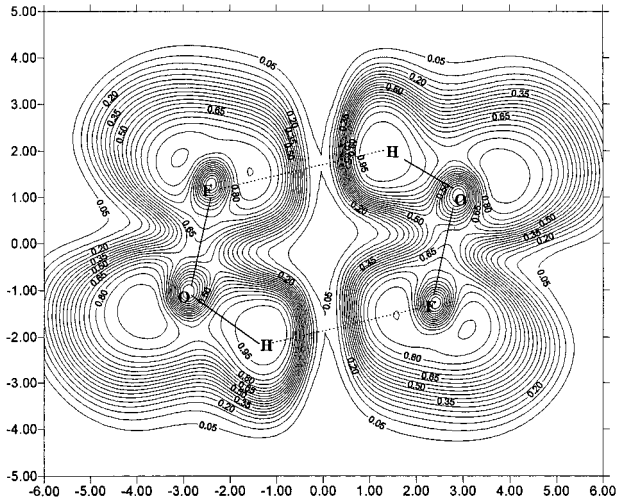

Figure 2. Two-dimensional representation of the ELF map for the $(HOF)_2$ complex with the cyclic conformation. The cutting plane between atoms was chosen. The spacing between adjacent lines is 0.05; lateral units are bohrs.

attractor between the core attractors of the atoms involved in the bond. The case of hydrogen is special because it has no core attractor and the above classification criteria cannot be applied.[45] This new topological analysis is in accord with the general ideas of chemical bonding, and ELF pictures are only slightly dependent on the quality of the used wave function—the ELF gradient field enjoys structural stability.

The computed basin populations ($\acute{N}$) of attractors localized in the linear and cyclic structures of $(HOF)_2$ are presented in Table 3.

The analysis of the two-dimensional representation of the ELF map, carried out for the $(HOF)_2$ dimer with the cyclic structure, is presented in Figure 2. One notices that there are no bonding attractors between fluorines and hydrogens, and hence, the interaction in the cyclic structure can by classified as an unshared-electron-type interaction. A similar result was obtained for the linear dimer, as well.

There is no charge transfer directly between the HOF monomers observed in the cyclic structure as given by the comparison of the respective sums of the ELF−basin populations. However, the $\acute{N}$ values show that some charge redistribution occurs within the hypofluorous acid subunits: the integrated densities over the F−O bonding disynaptic attractor basins are decreased about 0.1 e (with respect to the isolated HOF). This 10% depletion of the electron density over the F−O bonds is mainly compensated by an increase of the electron density of the fluorine nonbonding valence pairs. The basin populations of the $V_2(F_1)$ and $V_4(F_4)$ monosynaptic attractors are increased from 6.77 e in isolated HOF to 6.87 e in the dimer. The oxygen atoms are unaffected by this redistribution of the electron density, and the $\acute{N}$ values for the $V_1(O_2)$ and $V_3(O_5)$ monosynaptic attractors, which correspond to the oxygen lone pairs, change nominally by 0.01 e.

Similarly, the O−H bonds, described by the protonated disynaptic attractors $V_1(O_2,H_3)$ and $V_2(O_5,H_6)$, become slightly (by 0.02 e) electron-rich (1.80 e) when compared to the isolated HOF (1.78 e). Other small changes appear for the atomic core attractors $C_1(F_1)$ and $C_2(O_2)$ in which the basin populations differ by about 0.02 and 0.01 e, respectively. Therefore, the redistribution of the electron density in the cyclic $(HOF)_2$ complex can be understood as polarization of one subunit by the second subunit of the complex.

In the linear complex of $(HOF)_2$, the hypofluorous acid can act both as a Lewis acid and as a Lewis base. There is a charge transfer with the $H_3O_2F_1$ subunit donating electron density to the $H_6O_5F_4$ subunit. The difference of the respective sums of basin populations computed for attractors localized in both monomers shows a charge transfer of 0.03 e. In order to investigate the nature of this phenomenon, we compared the values of $\acute{N}$ given in Table 3. As expected, the two covalent O−F bonds are not equivalent. Considering the $H_3O_2F_1$ monomer, the F−O bond described by $V_3(F_1,O_2)$ disynaptic attractor expresses a decrease in basin population (0.27 e) by 0.15 e relative to the unperturbed HOF. Furthermore, the electron density of the O_2-H_3 bond, which is presented by the protonated disynaptic attractor $V_1(O_2,H_3)$, is reduced about 0.13 e. The partial accommodation of the redistributed electron density takes place over the regions of the oxygen and fluorine lone pairs. The integrated density for the $V_1(O_2)$ monosynaptic attractor basin corresponding to the electron lone pairs shows that the oxygen atom attracts most of the additional electron density (0.21 e). This effect can be explained by the role of the O_2 atom in the $O_2\cdots H_6-O_5$ hydrogen bond. Thus, only 0.08 e is shifted to the nonbonding valence pair of fluorine (F_1), when it is not incorporated in hydrogen bonding. The redistributions over the atomic cores are relatively small.

The situation for the $H_6O_5F_4$ subunit is different: while $H_3O_2F_1$ acts as a Lewis acid, the $H_6O_5F_4$ assumes the role of a Lewis base. The comparison with isolated HOF indicates that the electron density of the F_4-O_5 bond decreases similarly to the F_1-O_2 bond. The basin population over the $V_3(F_4,O_5)$ disynaptic attractor is about 0.05e smaller. However, the $\acute{N}$ value of 0.37 e is larger than the value of 0.27 e computed for the $H_3O_2F_1$ subunit and larger than the value of 0.32 e found for the cyclic structure. A possible explanation can be derived from the fact that H_3 and F_4 atoms are separated by 2.54 Å (MP2), which suggests that some interaction between these atom exists that additionally polarizes the F_4-O_5 bond.

The basin population over $V_2(O_5,H_6)$-protonated disynaptic attractor yields 1.85 e, which is 0.2 e larger then the value computed for $V_1(O_2,H_3)$. Furthermore, this population is 0.05 e larger than the value computed for the cyclic structure and 0.07 e larger than in isolated HOF. It can be associated with a

decrease of population of $V_3(O_5)$ lone pairs which donate electron density to the H_6-O_5 bond. In the case of the cyclic complex, the population of $V_3(O_5)$ lone pairs is almost unchanged and the explanation can be based on the fact that in the cyclic structure, the resulting redistribution of electron density in O−H bonds is balanced between interactions with two O−H···F hydrogen bonds. It is highly likely that in the linear dimer containing one strong O−H···O bond and a second very week O−H···F bond, the H···F interaction is too week to balance the O···HO interaction.

The result for the basin population, computed over the attractor of the fluorine lone electron pairs $V_4(F_4)$, yields a value of 6.83 e, which is about 0.02 e smaller than for $V_2(F_1)$ but it is still larger than the value of 6.77 e in unperturbed HOF. The comparison carried out for the $V_3(O_5)$ attractor basin reveals that there is a 0.25 e decrease of electron density at electron lone pairs at the O_5 atom with respect to $V_1(O_2)$. However, the population of 4.66 e of $V_3(O_5)$ is lower than the $V_1(O_2)$ population in isolated HOF (4.70 e). The redistributions of electron density over the atomic cores can be analyzed using the data from Table 3, where the nonequivalence of atomic cores is noticeable as well.

In conclusion, the above results show that in the linear system, a large amount of electron density is shifted from the free lone electron pairs of the O_5 atom and from the F_4-O_5 bond to the O_5-H_6 bond and the F_4 free lone electron pairs. This is in accord with the effect of polarization in the $O_5-H_6\cdots O_2$ hydrogen bond and the inductive role of fluorine. For the $H_3O_2F_1$ subunit, a slightly opposite effect is observed. For this subunit a larger depletion of electron density exists in the F_1-O_2 bond, but the main redistribution appears as a shift of electron density from the O_2-H_3 bond to the free lone electron pairs of F_1 and O_2.

Influence of a Dielectric Surrounding. One of the most important aspects of solvated molecules is their ability to shift their electronic distribution in response to an electric field generated by a perturbing system. To study this phenomenon for the $(HOF)_2$ species, the task of self-consistent reaction field (SCRF) computations[46] was undertaken. Full optimizations of the complexes were done within the self-consistent isodensity polarized continuum model (SCI-PCM) method using the B3LYP hybrid density functional with the 6-31G(d,p) basis set.

In the case of the cyclic dimer, the free energy of solvation (ΔF_{sol}) ($\epsilon = 2.0$) equals 1.29 kcal/mol at the B3LYP/6-31G-(d,p) level. For more polarized media, the ΔF_{sol} increases up to 3.32 kcal/mol (ϵ =10.0). Some selected geometrical parameters of the optimized cyclic structure with different dielectric constants are presented in Table 4. The obtained results suggest that the gain in the total energy in solution is almost entirely used to enforce the planarity of the complex (the new point group has C_{2h} symmetry) and to increase the intermolecular separation between the hypofluorous acid subunits. The complexation energy of the planar (C_{2h}) HOF dimer, with its geometry-optimized in solution ($\epsilon = 2.0$) but computed for the gas phase at the B3LYP/6-31G(d,p) level, equals −9.65 kcal/mol. This causes the planar form in the gas phase to be about 1 kcal/mol more stable than the linear (C_1) form and only about 0.2 kcal/mol less stable than the cyclic (C_2) one. The planarity of $(HOF)_2$ is reflected by the reduction of the dihedral angle O_2-F_1-H_6-O_5 defining the respective orientation of the HOF molecules from 23.9° (vacuum) to 0.0° (ϵ = 2, 4, 6, and 10). The valence angle, $H_6-O_5-F_4$, which describes the HOF subunit geometry, is negligibly changed, and for $\epsilon = 10.0$, the respective perturbation is 0.6°. The deviation from the linearity of the hydrogen bond as described by the $F_1-H_6-O_5$ angle (149.7° in vacuum) exhibits a strong dependence on the dielectric surrounding, and for $\epsilon = 2.0$, this angle increases to 154.2°. For a more polarized environment (ϵ = 4, 6, and 10), the angle gradually decreases, and for $\epsilon = 10.0$, a value of 152.9° was found.

TABLE 4: Most Relevant Geometrical Parameters[a] of Linear (C_1) and Cyclic (C_{2h}) Dimers of Hypofluorous Acid Computed at the B3LYP/6-31G(d,p) Level at Different Values of Dielectric Constant (ϵ)

param	unsolvated	$\epsilon = 2.0$	$\epsilon = 4.0$	$\epsilon = 6.0$	$\epsilon = 10.0$
		Linear (C_1) Dimer			
$d(F_1-O_2)$	1.4318	1.4318	1.4318	1.4317	1.4320
$d(O_2-H_3)$	0.9799	0.9792	0.9783	0.9778	0.9774
$d(O_2\cdots H_6)$	2.0123	2.0041	1.9726	1.9481	1.9103
$d(H_6-O_5)$	0.9831	0.9830	0.9832	0.9835	0.9841
$d(O_5-F_4)$	1.4434	1.4426	1.4417	1.4412	1.4403
$\angle F_1-O_2-H_3$	98.9	99.0	99.1	99.1	99.1
$\angle H_3-O_2-H_6$	79.0	83.3	8919	94.9	101.9
$\angle O_5-H_6-O_2$	138.8	142.1	146.0	150.0	156.1
$\angle F_4-O_5-I_6$	97.2	97.3	97.2	97.0	96.9
		Cyclic (C_{2h}) Dimer[b]			
$d(F_1-O_2)$	1.4444	1.4441	1.4438	1.4433	1.4438
$d(O_2-H_3)$	0.9820	0.9816	0.9813	0.9809	0.9812
$d(F_1\cdots H_6)$	1.8702	1.8834	1.8974	1.9055	1.9106
$\angle F_1-O_2-H_3$	97.2	97.7	97.8	97.9	97.9
$\angle O_2-H_3-F_4$	149.9	154.2	153.3	152.9	152.9
$\angle O_2-F_1-H_6$	102.6	108.1	109.0	109.2	109.2

[a] The bond distances are given in angstroms and the bond angles are given in degrees. [b] The unsolvated cyclic dimer has C_2 symmetry.

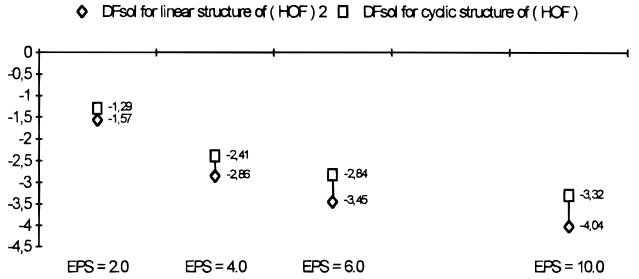

Figure 3. Comparison of the free energy of solvation (ΔF_{sol}) of the linear and cyclic structures of $(HOF)_2$ in solution. The parameter ΔF_{sol} is defined as $\Delta F_{sol}^{structure} = E^{structure}(vacuum) - E^{structure}(solution)$, where $E^{structure}$ is a total energy computed at the B3LYP/6-31G(d,p) level. The vertical energy scale is in kcal/mol, and the horizontal scale is values of the dielectric constant (ϵ).

The length of the hydrogen bond, $d(F_1\cdots H_6)$, is increaased in solution by 0.0091 Å ($\epsilon = 2.0$). For a more dielectric surrounding, $d(F_1\cdots H6)$ gradually lengthens from 1.8834 (ϵ = 2.0) to 1.9106 Å ($\epsilon = 10.0$). For the two intramolecular valence bonds $d(H_3-O_2)$ and $d(O_2-F_1)$ a very small shortenings of the bond distances is noted for a dielectric surrounding of $\epsilon = 2.0$. Similarly, for larger dielectric constants, only very small changes could be found.

The calculations of the vibrational frequencies predict that the cyclic complex is not a local minimum but a saddle point in solution. For $\epsilon = 2.0$, one imaginary frequency ($\nu_1 = 37.9$i) appears, and a small decrease of this frequency can be observed for other values of the dielectric constants as well.

The linear $(HOF)_2$ complex is more stable in solution than the cyclic complex. This can be seen also in the ΔF_{sol} values for the two complex structures plotted in Figure 3. As expected, both structures are stabilized by the dielectric environment, but while in the vacuum, the energy difference is just a few tenths of kcal mol^{-1}, and stronger electrostatic effects of the medium stabilize the linear structure more than the cyclic dimer. The additional stabilization of the linear conformer can also be seen from Table 4, representing the structural parameters for the

TABLE 5: Computed Vibrational Frequencies (ν, in cm^{-1}) and Frequency Shifts ($\Delta\nu$, in cm^{-1}) with the B3LYP/6-31G(d,p) Method in Different Environments for the Monomer and the Linear Dimer

	vacuum		$\epsilon = 2.0$		$\epsilon = 4.0$		$\epsilon = 6.0$		$\epsilon = 10.0$		
	ν	$\Delta\nu$	ν	$\Delta\nu$	ν	$\Delta\nu$	ν	$\Delta\nu$	ν	$\Delta\nu$	approx assignment
						Monomer					
ν_1[a]	3733.3		3736.7		3741.5		3744.1		3741.6		OH str
ν_2	1396.8		1398.9		1398.9		1399.5		1399.0		FOH bend
ν_3	998.2		997.7		995.2		995.4		993.9		OF str
						Dimer					
ν_1[a]	3664.3	−69.0	3679.1	−57.6	3699.3	−42.2	3712.0	−32.1	3719.1	−22.5	O_2H_3 str
ν_2	3583.5	−149.8	3586.4	−150.3	3582.1	−159.4	3574.0	−170.1	3560.5	−181.1	O_5H_6 str
ν_3	1489.7	92.9	1475.3	76.4	1465.9	67.0	1461.8	62.3	1461.9	62.9	$F_4O_5H_6$ bend
ν_4	1416.0	19.2	1407.0	8.1	1395.1	−3.8	1390.9	−8.6	1388.7	−10.3	$F_1O_2H_3$ bend
ν_5	1994.4	6.2	1003.8	6.1	1003.3	8.1	1003.3	7.9	1002.0	8.1	F_1O_2 str
ν_6	976.4	−21.8	978.1	−19.6	981.0	−14.2	983.0	−12.4	986.1	−7.8	F_4O_5 str
ν_7[b]	558.6		493.1		464.2		466.8		480.7		$F_4O_5H_6$ wag
ν_8	433.0.		413.4		368.5		341.4		333.0		$F_1O_2H_3$ wag
ν_9	211.2		188.6		191.8		196.0		205.4		$F_4O_5H_6$ wag
ν_{10}	194.0		173.6		118.1		85.3		76.2		$F_1O_2H_3$ wag
ν_{11}	69.6		62.3		65.6		66.3		38.4		intermolec str
ν_{12}	61.6		59.8		38.4		36.4		7.5		torsion

[a] Intramolecular modes. [b] Intermolecular modes.

dimer including a dielectric environment. The $O_2\cdots H_6$ intermolecular distance is decreased by 0.0082 Å from the unsolvated value of 2.0123 Å at the B3LYP/6-31G(d,p) level of theory. The immersion in a solution with higher values of dielectric constants reduces $d(O_2\cdots H_6)$ from 1.9726 ($\epsilon = 4.0$) to 1.9103 Å ($\epsilon = 10.0$). Also, the effect of the solvent on the length of the intermolecular H bond is different for the F···H and O···H types of interactions. There is an elongation of the $d(F_4\cdots H_3)$ distance and a contraction of the $d(O_2\cdots H_6)$ bond distance. This effect is smaller for the O···H interaction (0.0082 Å) than for the F···H one (0.0091 Å) using $\epsilon = 2.0$, but a reverse order is observed for a high dielectric constant of $\epsilon = 10.0$, where this effect is larger for the O···H interaction (0.1020 Å) than for the F···H interaction (0.0363 Å). The O_5-F_4 and O_2-F_1 valence bonds undergo only small changes, as shown in Table 4. In fact, the O_5-H_6 bond, where the H_6 atom is involved in the $O_2\cdots H_6-O_5$ hydrogen bond, shows a nominal shortening of 0.0001 Å with a small dielectric constant ($\epsilon = 2.0$) and a slightly larger shortening of 0.001 Å at $\epsilon = 10.0$.

A comparison of the valence angles which describe the internal geometry of the FOH subunits reveals very small changes for the $F_1-O_2-H_3$ ($F_4-O_5-H_6$) angles. For $\epsilon = 10.0$, these angles deviate only by 0.1° from the values calculated for the unsolvated species at the same level of theory. The $O_2-H_6-O_5$ angle, which defines the hydrogen bridge bond, shows a tendency toward increased linearity. For $\epsilon = 2.0$, this angle is 3.3° larger than that found in vacuum (138.8°). In more polar media, this angle is enlarged to 146.0°, 149.8°, and 156.1° with $\epsilon = 4.0$, 6.0, and 10.0, respectively.

The solvent effect on the vibrational frequencies of the monomer and the linear HOF dimer is presented in Table 5. The IR spectra are very sensitive to the values of the dielectric constant which characterize the surrounding. An increase of the polarity of a solvent decreases the O_5-H_6 stretching frequency and increases, the O_2H_3 stretching frequency. For the $F_4O_5H_6$ bending mode, the blue shift is diminished with an increase in the polarity of the environment. Interesting changes are noted for the $F_1O_2H_3$ bending modes. Depending on the polarity of the solvent, either a red or a blue shift is found. Although for vacuum and $\epsilon = 2.0$ blue shifts of 19.2 and 8.1 cm^{-1}, respectively are observed, for a more polarized surrounding ($\epsilon = 4$, 6, and 10) a gradual increase of the red shift is found, which for $\epsilon = 10.0$ becomes −10.3 cm^{-1}. For the intramolecular F_4O_5 stretching mode, relatively large red shifts are predicted, ranging from 21.8 cm^{-1} in vacuum to 7.8 cm^{-1} for $\epsilon = 10.0$.

Finally, similar trends are noted for almost all intermolecular modes of the dimer. With an increase of the polarity of the dielectric surrounding, the frequencies of all modes strongly decrease. This behavior is especially pronounced for the $F_1O_2H_3$ wagging, the intermolecular stretching, and the torsion modes.

As was mentioned in the Introduction, Appelman et al.[17] identified the HOF dimer in the Ar, N_2, O_2, and CH_4 matrices. Except for absorptions corresponding to $(HOF)_3$ and higher oligomers, they found two bands for $(HOF)_2$ in the O−H stretching region at ca. 3490−3553 and 3462−3481 cm^{-1} and an absorption in the H−O−F deformation region at 1365−1396 cm^{-1}. These absorptions were assigned to the linear conformer of $(HOF)_2$. A graphical comparison of the computed spectra and the spectra of $(HOF)_2$ taken from the Appelman et al. paper[17] are displayed in Figure 4. One notices the excellent agreement within the deformation region where the observed absorption at 1395 cm^{-1} in the Ar matrix is very close to the calculated value of ν_4 (1395.1 cm^{-1}) computed with $\epsilon = 4.0$ or ν_4 (1407.0 cm^{-1}) computed with $\epsilon = 2.0$. The O−H stretching region is less precisely predicted by our computations, and the respective difference between the computed and experimentally measured frequencies ranges from 30 to 90 cm^{-1}. However, one distinct difference of the calculated vibrational bands between the cyclic and the linear conformers of $(HOF)_2$ can be found in favor of the assignement of the $(HOF)_2$ absorptions in solid Ar as the linear conformer. As shown in Figure 5, the cyclic conformer of $(HOF)_2$ shows only one band in the ν_{OH} region as well as in the H−O−F bending region at ca. 1400 cm^{-1}. Instead, the linear conformer of $(HOF)_2$ induces a doublet in these regions in accordance with the experimental evidence from low-temperature matrices.[17] Also, the far-infrared region shown in Figure 5 would make a nice fingerprint region for the different conformers of $(HOF)_2$ due to the large intensity of these intermolecular vibrational modes. The second absorptions observed by Appelman et al.[17] in the O−H stretching region, i.e., 3462−3481 cm^{-1}, and attributed to the $(HOF)_n$ species have no counterpart in our computed spectra. Hence, we agree that it probably belongs to a higher oligomer mode.

At this point, some remarks can be made on the calculated properties of the $(HOF)_2$ dimer. The two structures of the hydrogen-bonded dimers of $(HOF)_2$ are almost equally feasible in the gas phase. After immersion in solutions, some kind of "phase transition" is observed where the cyclic dimer becomes unstable. This change of the structural stability is reflected by the presence of one imaginary frequency appearing when a

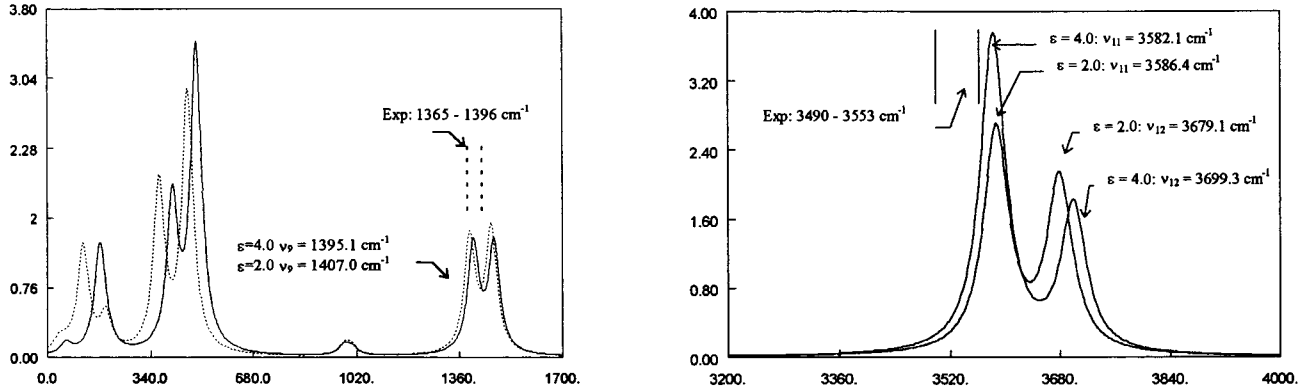

Figure 4. Comparison of the synthetic IR spectra calculated for linear (C_1) conformation of $(HOF)_2$ at the B3LYP/6-31G(d,p) level using the self-consistent isodensity polarized continuum model (SCI-PCM) approximation of solution with dielectric constants of $\epsilon = 2.0$ (solid line) and 4.0 (dotted line). The experimental results of Appelman et al.[17] are denoted as the area between two vertical lines. The synthetic IR spectra were prepared with the SYNSPEC program of Karl K. Irikura, National Institute of Standards and Technology, Gaithersburg, MD.

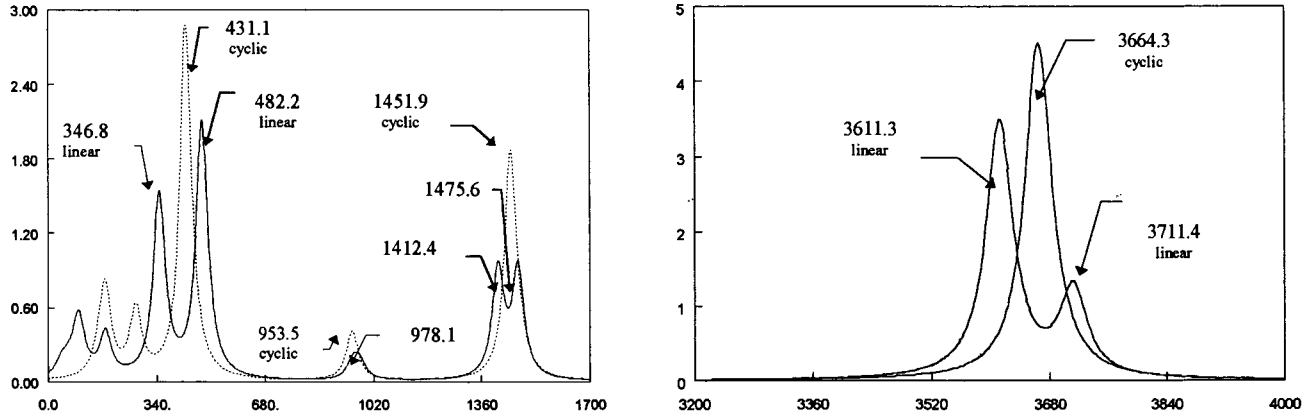

Figure 5. Comparison of the synthetic IR spectra of the linear (C_1) and cyclic (C_2) conformations of $(HOF)_2$ computed at the B3LYP/6-311++G-(2d,2p) level in vacuum in spectral regions below 1700 and between 3200 and 4000 cm^{-1}. Frequencies are given in cm^{-1}, and intensities are given in km/mol.

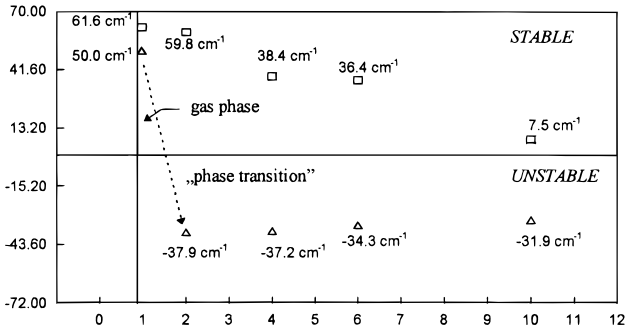

Figure 6. Dependence of the structural stability implied by an occurring or lack of imaginary vibrational frequency on the dielectric constant used to represent the solution computed for linear (squares) and cyclic (triangles) structures. The dotted arrow emphasizes the predicted unstability of the cyclic dimer. The horizontal scale corresponds to values of the dielectric constant. The vertical scale represents the lowest torsional vibrational frequency given in cm^{-1}.

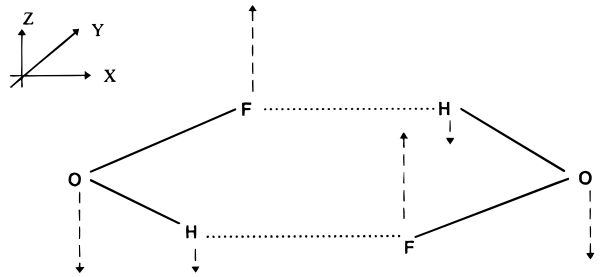

Figure 7. Transition vector of the imaginary vibrational mode of the cyclic conformation of the $(HOF)_2$ complex immersed in solution.

dielectric environment is introduced, which indicates the transition-state nature of this stationary point on the potential energy surface. A comparison of the cyclic conformer with the linear form is presented in Figure 6. The analysis of the transition vector shown in Figure 7 suggests that the lowest frequency mode corresponds to a deformation of the planar, cyclic form to the nonplanar conformation resembling the linear one. Furthermore, one can see that "the structural stability" of the linear dimer diminishes very fast and that for highly polarized solutions, both complexes should exhibit one imaginary frequency. Therefore, the existence of a new geometry of $(HOF)_2$ is possible for values of ϵ higher than those considered in this computational study.

The crystal structure data of solid HOF indicated infinite HOF chains with O···H−O hydrogen bonds.[18] This linear rearrangement is consistent with our computationally predicted stability of the linear $(HOF)_2$ dimer. Although the geometry of the linear conformation predicted by calculations differs from the crystal structure with almost linear O···H−O hydrogen bonds and the fluorine atoms located in trans positions, the increased polarizability of the solution seems to enforce linearity of the H-bridge bond for the linear $(HOF)_2$ conformer. Furthermore, studies on molecular packing in crystalline systems clearly show that hydrogen bond accepting properties of functional groups depend on the local intramolecular environment.[47] Therefore, the geometry of the infinite chain $(HOF)_\infty$ may result in

additional stabilization of the system and a geometry of $(HOF)_2$ different from that found in the unsolvated state.

To our knowledge, the dielectric constant of the crystal of hypofluorous acid is unknown. Hence, it is difficult to draw any precise conclusions about the possible geometry of HOF oligomers in the solid state using data computed for $(HOF)_2$ in solution. However, we believe that further computational studies (for instance, molecular dynamics or Monte Carlo simulations) starting from our molecular geometry of the linear dimer with O···H−O and F···H−O hydrogen bonds might give some additional view on other possible structures of HOF aggregation in the crystalline state. It is worth pointing out that crystalline HF does not undergo any phase transitions up to its melting point due to the very strong hydrogen bonds between the HF monomers. On the contrary, there are several phase transitions in ice (H_2O), and therefore, it is suspected that for HOF, which could be regarded as an intermediate between HF and HOH, several phase transitions might possibly occur.

IV. Summary

For the $(HOF)_2$ dimers, two geometries are found for the gas phase that are almost equally possible: the cyclic (C_2) conformer with F···H−O and the linear (C_1) conformer with O···H−O and F···H−O hydrogen bonds. The binding energies are predicted to be 2.16 and 2.50 kcal/mol, respectively, at the CCSD(T)/6-311++G(2d,2p)//MP2/6-311++G(2d,2p) level of theory.

The analysis of the interaction based on the electron localization function revealed a shift of the electron density from the F−O bonds to the regions of the free, valence, electron pairs located at the fluorine atoms in the cyclic $(HOF)_2$. In the linear $(HOF)_2$ dimer, there is an electron transfer of 0.03 e between the HOF monomers.

The computations, including a polarizable surrounding, indicate that the cyclic structure with a the planar geometry (C_{2h}) is unstable (a transition state), whereas the linear structure is still stable. A comparison with the available experimental IR data of $(HOF)_2$ from the low-temperature matrices shows good agreement with the computed frequencies.

Acknowledgment. S.B. and Z.L gratefully acknowledge the Wrocław Supercomputer Center, Poznań Supercomputer Center, and Interdisciplinary Centre for Mathematical and Computational Modeling in Warsaw for providing the computer time and facilities where some of the calculations were performed. Furthermore, we are grateful to Prof. B. Silvi (Université Pierre et Marie Curie, France) for his assistance with the ELFGTO program, as well as discussion of the results from topological analysis of the electron localization function. The CSC Center for Scientific Computing Ltd. (Espoo, Finland) is thanked for the computer time used on the CREY C94 and SGI Power-Challenge supercomputers. J. Lundell gratefully acknowledges financial support from the Finnish Cultural Foundation. J. Leszczyński acknowledges the Mississippi Center for Supercomputing Research for generous allotment of computer time for the part of the calculations presented here.

References and Notes

(1) Elliott, S. *Atmos. Environ.* **1983**, *17*, 759.

(2) Solomon, S.; Garsia, R. R.; Rowland, F. S.; Weubles, D. J. *Nature* **1986**, *321*, 755.

(3) Anderson, J. G. *Annu. Rev. Phys. Chem.* **1987**, *38*, 489.

(4) Hanson, D. R.; Ravishankara, A. R. *J. Phys. Chem.* **1992**, *96*, 2682.

(5) Abbot, J. P. D.; Malina, M. J. *J. Phys. Chem.* **1992**, *96*, 7074.

(6) Paulet, G.; Pirre, M.; Maguin, F.; Ramaroson, R.; Le Brass, G. *Geophys. Res. Lett.* **1992**, *19*, 2305.

(7) Fan, S.-M.; Jacob, D. L. *Nature* **1992**, *359*, 522.

(8) Hassanzadeh, P.; Irikura, K. K. *J. Phys. Chem. A* **1997**, *101*, 1581 and references cited therein.

(9) Rozen, S.; Bareket, Y. *J. Org. Chem.* **1997**, *62*, 1457.

(10) Rozen, S. *Chem. Rev.* **1996**, *96*, 1717.

(11) Dunkelberg, O.; Haas, A.; Klapdor, M. F.; Mootz, D.; Poll, W.; Appelman, E. H. *Chem. Ber.* **1994**, *127*, 1871.

(12) Appelman, E. H.; Kim, H. *J. Chem. Phys.* **1972**, *57*, 3272. Goleb, J. A.; Classen, H. H.; Studier, M. H.; Appelman, E. H. *Spectrochim. Acta, Part A* **1972**, *28A*, 65.

(13) Kim, H.; Pearson, E. F.; Appelman, E. H. *J. Chem. Phys.* **1972**, *56*, 1.

(14) Berkowitz, J.; Dehmer, J. L.; Appelman, E. H. *Chem. Phys. Lett.* **1973**, *19*, 334.

(15) Berkowitz, J.; Appelman, E. H.; Chupka, W. A. *J. Chem. Phys.* **1973**, *58*, 1950.

(16) Hindman, J. C.; Svirmickas, A.; Appelman, E. H. *J. Chem. Phys.* **1972**, *57*, 4542.

(17) Appelman, E. H.; Downs, A. J.; Gardner, C. J. *J. Phys. Chem.* **1989**, *93*, 598.

(18) Poll, W.; Pawelke, G.; Mootz, D.; Appelman, E. H. *Angew. Chem., Phys. Int. Ed. Engl.* **1988**, *27*, 392.

(19) Appelman, E. H.; Wilson, W. W.; Kim, H. *Spectrochim. Acta, Part A* **1981**, *37A*, 385.

(20) Kim, H.; Appelman, E. H. *J. Chem. Phys.* **1982**, *76*, 1664.

(21) Christe, K. O. *J. Fluorine Chem.* **1987**, *35*, 621.

(22) Kim, H.; Sabin, J. R. *Chem. Phys. Lett.* **1973**, *20*, 215.

(23) Berski, S.; Silvi, B.; Latajka, Z.; Leszczynski, J. To be published.

(24) Allred, A. L.; Rochow, E. G. *J. Inorg. Nucl. Chem.* **1958**, *5*, 264.

(25) Silvi, B. Private communication.

(26) Johansson, A.; Kollman, P. A.; Liebman, J. F.; Rothenberg, S. *J. Am. Chem. Soc.* **1974**, *96*, 3750.

(27) Alcamí, M.; Mó, O.; Yáñez, M.; Abboud, Jose-Luis M.; Elguero, J. *Chem. Phys. Lett.* **1990**, *172*, 471.

(28) Burk, P.; Koppel, I. A.; Rummel, A.; Trummal, A. *J. Phys. Chem.* **1995**, *99*, 1432.

(29) Silvi, B.; Savin, A. *Nature* **1994**, *371*, 683.

(30) Becke, A. D. *Phys. Rev. A* **1988**, *38*, 3098.

(31) Lee, C.; Yang, W.; Paar, R. G. *Phys. Rev. B* **1988**, *37*, 785.

(32) Hariharan, P. C.; Pople, J. A. *Theor. Chim. Acta* **1973**, *28*, 213.

(33) Frisch, M. J.; Pople, J. A.; Binkley, J. S. *J. Chem. Phys.* **1984**, *80*, 3265.

(34) Boys, S. F.; Bernardi, F. *Mol. Phys.* **1970**, *19*, 553.

(35) Frisch, M. J.; Trucks, G. W.; Schlegel, H. B.; Gill, P. M. W.; Johnson, B. G.; Robb, M. A.; Cheeseman, J. R.; Keith, T. A.; Petersson, G. A.; Montgomery, J. A.; Raghavachari, K.; AI-Laham, M. A.; Zakrzewski, V. G.; Ortiz, J. V.; Foresman, J. B.; Cioslowski, J.; Stefanov, B.; Nanayakkara, A.; Challacombe, M.; Peng, C. Y.; Ayala, P. Y.; Chen, W.; Wong, M. W.; Andres, J. L.; Replogle, E. S.; Gomperts, R.; Martin, R. L.; Fox, D. J.; Binkley, J. S.; Defrees, D. J.; Baker, J.; Stewart, J. P.; Head-Gordon, M.; Gonzalez, C.; Pople, J. A. GAUSSIAN 94, Gaussian, Inc., Pittsburgh, PA, 1995.

(36) Silvi, B. ELFGTO program, Paris, 1996, private communication.

(37) Glukhovtsev, M. N.; Pross, A.; Radom, L. *J. Phys. Chem.* **1996**, *100*, 3498.

(38) Xantheas, S. S. *J. Chem. Phys.* **1996**, *104*, 8821.

(39) Novoa, J. J.; Planas, M.; Rovira, M. C. *Chem. Phys. Lett.* **1996**, *251*, 33.

(40) Lee, T. J.; Rice, J. E.; Dateo, C. E. *Mol. Phys.* **1996**, *89*, 1359.

(41) Chirlian, L. E.; Francl, M. M. *J. Comp. Chem.* **1987**, *8*, 894.

(42) Bader, R. F. W.; Nguyen-Dang, T. T.; Tal, Y. *Rep. Prog. Phys.* **1981**, *44*, 895.

(43) Becke, A. D.; Edgecombe, K. E. *J. Chem. Phys.* **1990**, *92*, 5397.

(44) Bader, R. F. W. *Atoms in Molecules: A Quantum Theory;* Oxford University: Cambridge, 1990.

(45) Silvi, B. *Description topologique de la liaison chimique;* Paris, 1996.

(46) Foresman, J. B.; Frisch, A. E. *Exploring Chemistry with Electronic Structure Methods*, 2nd ed.; Gaussian, Inc.: Pittsburgh, PA, 1995−1996 and references cited within.

(47) Böhm, H-J.; Brode, S.; Hesse, U.; Klebe, G. *Chem. Eur. J.* **1996**, *2*, 1509.

(48) Rock, S. L.; Pearson, E. F.; Appelman, E. H.; Norris, C. L.; Flygare, W. H. *J. Chem. Phys.* **1973**, *59*, 3440.